

## PML ABSORBING BOUNDARY CONDITIONS FOR THE MULTIREOLUTION TIME-DOMAIN TECHNIQUES BASED ON THE DISCRETE WAVELET TRANSFORM

C. Represa (\*), C. Pereira (\*), A.C.L. Cabeceira (\*\*), I. Barba (\*\*), J. Represa (\*\*)

(\*) Dpt. of Electromechanical Engineering, University of Burgos, 09001 Burgos, Spain

Phone: +34 947258830 FAX: +34 947258831 E-Mail: [crepresa@ubu.es](mailto:crepresa@ubu.es)

(\*\*) Dpt. of Electricity and Electron, University of Valladolid, 47011 Valladolid, Spain

Phone: +34 983423223 FAX: +34 983423225 E-Mail: [ibarba@ee.uva.es](mailto:ibarba@ee.uva.es)

**Abstract:** The use of numerical methods to solve electromagnetic problems with open boundaries requires a method to limit the domain in which the field is computed. This can be achieved by truncating the mesh and setting certain numerical boundary conditions on the outer perimeter of the domain to simulate its extension to infinity. In this paper, the formulation of the perfectly matched layer (PML) is applied to the multiresolution time-domain technique (MRTD) to effectively simulate free-space. The PML region is modelled by means of the two-dimensional discrete wavelet transform. In addition, the numerical reflectivity of the PML medium is also investigated for a variety of thicknesses.

**Keywords:** Absorbing boundary conditions, PML, MRTD, DWT.

### 1. INTRODUCTION

Different wavelet-based discretizations for Maxwell equations have been developed in the very recent literature. These numerical methods are known as multiresolution time-domain (MRTD) techniques and its main point of interest is the intrinsic capability of wavelets to add higher spatial frequency contributions in the representation of the fields. These methods employ numerical analysis based on different wavelet functions like Battle-Lemarié [1], Haar [2], and Daubechies [3], and have been applied to several electromagnetic problems such as scattering, radiation, and integrated-circuit component modeling. Many of these applications involve modeling electromagnetic fields in an unbounded open space. It is well known that, since the computational domain is limited in space by storage limitations, a certain type of boundary condition, which is called absorbing boundary condition (ABC) must be implemented to effectively simulate open regions and having the capability to suppress numerical reflections of the outgoing waves.

Many absorbing boundary conditions have been proposed in past years [4]-[6], but since 1994, a new improvement has been made in this area by J.P. Berenger's technique designated as the perfectly matched layer or PML [7]. This technique is based on the introduction of a highly effective absorbing material medium to terminate the outer boundary of the space lattice. This nonphysical absorbing medium has a wave impedance less sensitive to the angle of incidence, polarization and frequency of outgoing waves, and therefore a perfectly matched interface is derived.

In this paper, the PML principle has been implemented into the multiresolution time-domain technique. This technique uses Daubechies compactly supported wavelet functions denoted as  $D_M$  [8], and the PML medium has been modelled using the discrete wavelet transform (DWT).

### 2. APPLICATION OF THE PML ABSORBER TO THE MRTD TECHNIQUE

#### *A. Fundamentals of the PML theory*

In the PML theory described in [7] it is assumed that the PML region is characterized by a free-space permittivity  $\epsilon_0$  and permeability  $\mu_0$ , and electric and magnetic conductivities  $\sigma$  and  $\sigma^*$ , respectively. Then, if the following PML relationship is satisfied

$$\frac{\sigma}{\epsilon_0} = \frac{\sigma^*}{\mu_0} \quad (1)$$

the impedance of the medium matches that of vacuum and no reflection occurs when a plane wave propagates normally across a vacuum-medium interface. Since sharp variations of conductivity can create numerical reflections, for a PML region of thickness  $\delta$ , the conductivities are chosen to vary

from zero at the vacuum-layer interface to a maximum value  $\sigma_{MAX}$  at the outer side of the layer

$$\sigma(\rho) = \sigma_{MAX} \left(1 - \frac{\rho}{\delta}\right)^n, \text{ with } n = 2 \text{ for } 0 \leq \rho \leq \delta. \quad (2)$$

Usually the PML area is terminated with a PEC, thus the maximum value  $\sigma_{MAX}$  is determined by a designated apparent reflection coefficient  $R$  at normal incidence, which is given by the relationship [7]

$$R = \exp\left(-\frac{2\sigma_{MAX}\delta}{\varepsilon_0 c(n+1)}\right). \quad (3)$$

By choosing the theoretical reflection coefficient (typically  $R = 10^{-4}$  or  $R = 10^{-5}$ ) and the PML thickness  $\delta$ , the maximum value  $\sigma_{MAX}$  can be obtained from (3).

### B. Implementation of the PML absorber

In this section, we will analyze the implementation of the PML absorber into the MRTD scheme. This implementation does not involve a special treatment if scaling functions are used to expand the field components. Otherwise, if two or more resolution levels are applied, that is, scaling and wavelet functions are used to expand the field components, we must model the PML medium before its implementation into the algorithm. For simplicity in this presentation, let us assume a one dimensional problem. That is, the simplest case of a TEM plane wave propagating in free-space, with  $E_x$  and  $H_y$  fields, is considered. In order to simulate open boundaries, we will locate two PML areas of thickness  $\delta$  at both ends, with an electric conductivity  $\sigma$  and a magnetic conductivity  $\sigma^*$  satisfying the relation (1) and with a parabolic spatial distribution, that is, a spatial profile like (2) with  $n = 2$  (Fig. 1). Within the PML area, the equations to

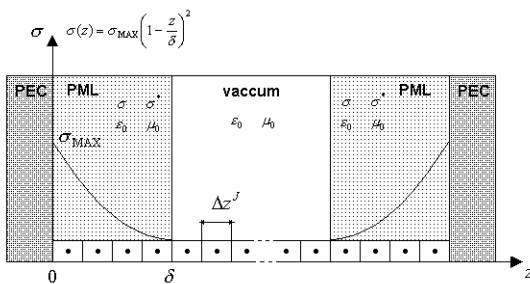


Fig. 1. Parabolic spatial distribution of  $\sigma$  and  $\sigma^*$  within the PML area.

solve are

$$\frac{\partial H_y}{\partial t} + \frac{\sigma^*}{\mu_0} H_y = -\frac{1}{\mu_0} \frac{\partial E_x}{\partial z} \quad (4.a)$$

$$\frac{\partial E_x}{\partial t} + \frac{\sigma}{\varepsilon_0} E_x = -\frac{1}{\varepsilon_0} \frac{\partial H_y}{\partial z}. \quad (4.b)$$

Thus, according to the exponential time stepping [9], these equations are discretized in time as

$$H_y^{n+\frac{1}{2}} = e^{-\frac{\sigma^* \Delta t}{\mu_0}} H_y^{n-\frac{1}{2}} - \frac{1}{\sigma^*} \left(1 - e^{-\frac{\sigma^* \Delta t}{\mu_0}}\right) \frac{\partial E_x^n}{\partial z} \quad (5.a)$$

$$E_x^{n+1} = e^{-\frac{\sigma \Delta t}{\varepsilon_0}} E_x^n - \frac{1}{\sigma} \left(1 - e^{-\frac{\sigma \Delta t}{\varepsilon_0}}\right) \frac{\partial H_y^{n+\frac{1}{2}}}{\partial z}. \quad (5.b)$$

According to the notation given in [8], an approximate solution at level  $J$  can be obtained using scaling functions of  $J$ -th order to expand each field component respect to space. The final set of discretized equations are expressed in matrix form as follows

$${}^{n+\frac{1}{2}}[H^\phi]^J = [\sigma_1^*]^J {}^{n-\frac{1}{2}}[H^\phi]^J - [\sigma_2^*]^J \frac{1}{\Delta z} [d^J]^n [E^\phi]^J \quad (6.a)$$

$${}^{n+1}[E^\phi]^J = [\sigma_1]^J {}^n[E^\phi]^J - [\sigma_2]^J \frac{1}{\Delta z} [d^J]^{n+\frac{1}{2}} [H^\phi]^J \quad (6.b)$$

where  ${}^n[H^\phi]^J$  and  ${}^n[E^\phi]^J$  are column vectors whose elements are the scaling coefficients at level  $J$ , evaluated at time  $t = n\Delta t$ , of the magnetic and electric field expansions, respectively. The matrix  $[d^J] = \mathbf{D}^J$  is the derivative matrix at level  $J$  (Fig. 2) [8].

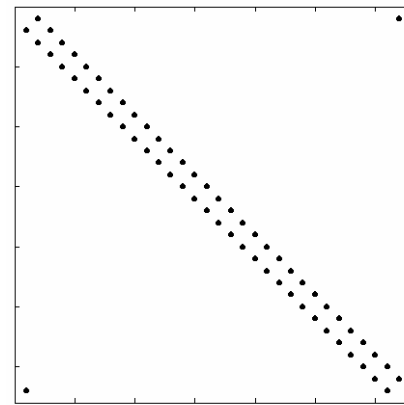


Fig. 2. Derivative matrix  $D^J$ : Only non zero elements have been plotted.

The matrices  $[\sigma_1]^J$ ,  $[\sigma_2]^J$ ,  $[\sigma_1^*]^J$ , and  $[\sigma_2^*]^J$  are diagonal matrices whose elements are function of the time discretization interval  $\Delta t$ , the permittivity  $\epsilon_0$ , the permeability  $\mu_0$ , and the electric and magnetic conductivity,  $\sigma$  and  $\sigma^*$ , respectively, and are distinct from zero only at each point  $z = k\Delta z^J = k2^{-J}\Delta z$  within the PML area of thickness  $\delta = L\Delta z^J$ . These matrices are given by the set of equations (7.a) to (7.d).

Now, the spatial resolution can be increased by adding wavelet functions to the field expansion. Therefore, adding wavelet functions of  $J$ -th order to

the field expansion results in an approximate solution at level  $J+1$  with a spatial discretization interval  $\Delta z^{J+1}$ . The formulation of the fields within the PML region is written in matrix form as indicated in equation (8.a) and equation (8.b), where a derivative matrix at level  $J+1$  ( $\mathbf{D}^{J+1}$ ) [8] has been used, and the matrices related to the conductivity of the PML medium have been modeled using the two-dimensional discrete wavelet transform  $\text{DWT}_{2D}$  [10].

$$[\sigma_1]^J = \begin{bmatrix} \sigma_{10}^J & & & & \\ & \ddots & & & \\ & & \sigma_{1k}^J & & \\ & & & \ddots & \\ & & & & \sigma_{1L-1}^J \end{bmatrix}, \text{ where } \sigma_{1k} = \exp\left(-\frac{\sigma(k\Delta z^J) \cdot \Delta t}{\epsilon_0}\right) \quad (7.a)$$

$$[\sigma_2]^J = \begin{bmatrix} \sigma_{20}^J & & & & \\ & \ddots & & & \\ & & \sigma_{2k}^J & & \\ & & & \ddots & \\ & & & & \sigma_{2L-1}^J \end{bmatrix}, \text{ where } \sigma_{2k} = \frac{1}{\sigma(k\Delta z^J)} \left(1 - \exp\left(-\frac{\sigma(k\Delta z^J) \cdot \Delta t}{\epsilon_0}\right)\right) \quad (7.b)$$

$$[\sigma_1^*]^J = \begin{bmatrix} \sigma_{10}^{*J} & & & & \\ & \ddots & & & \\ & & \sigma_{1k}^{*J} & & \\ & & & \ddots & \\ & & & & \sigma_{1L-1}^{*J} \end{bmatrix}, \text{ where } \sigma_{1k}^* = \exp\left(-\frac{\sigma^*(k\Delta z^J) \cdot \Delta t}{\mu_0}\right) \quad (7.c)$$

$$[\sigma_2^*]^J = \begin{bmatrix} \sigma_{20}^{*J} & & & & \\ & \ddots & & & \\ & & \sigma_{2k}^{*J} & & \\ & & & \ddots & \\ & & & & \sigma_{2L-1}^{*J} \end{bmatrix}, \text{ where } \sigma_{2k}^{*J} = \frac{1}{\sigma^*(k\Delta z^J)} \left(1 - \exp\left(-\frac{\sigma^*(k\Delta z^J) \cdot \Delta t}{\mu_0}\right)\right). \quad (7.d)$$

$${}^{n+\frac{1}{2}} \begin{bmatrix} H^\phi \\ H^\psi \end{bmatrix}^{J+1} = \begin{bmatrix} d \sigma_1^* & \gamma \sigma_1^* \\ \beta \sigma_1^* & \alpha \sigma_1^* \end{bmatrix}^{n-\frac{1}{2}} \begin{bmatrix} H^\phi \\ H^\psi \end{bmatrix}^{J+1} - \begin{bmatrix} d \sigma_2^* & \gamma \sigma_2^* \\ \beta \sigma_2^* & \alpha \sigma_2^* \end{bmatrix} \frac{1}{\Delta z} \begin{bmatrix} d^J & \gamma^J \\ \beta^J & \alpha^J \end{bmatrix}^n \begin{bmatrix} E^\phi \\ E^\psi \end{bmatrix}^{J+1} \quad (8.a)$$

$${}^{n+1} \begin{bmatrix} E^\phi \\ E^\psi \end{bmatrix}^{J+1} = \begin{bmatrix} d \sigma_1 & \gamma \sigma_1 \\ \beta \sigma_1 & \alpha \sigma_1 \end{bmatrix}^n \begin{bmatrix} E^\phi \\ E^\psi \end{bmatrix}^{J+1} - \begin{bmatrix} d \sigma_2 & \gamma \sigma_2 \\ \beta \sigma_2 & \alpha \sigma_2 \end{bmatrix} \frac{1}{\Delta z} \begin{bmatrix} d^J & \gamma^J \\ \beta^J & \alpha^J \end{bmatrix}^{n+\frac{1}{2}} \begin{bmatrix} H^\phi \\ H^\psi \end{bmatrix}^{J+1} \quad (8.b)$$

The procedure depicted in Fig. 3 to obtain these matrices is as follows: first, we compute the  $\sigma$ -matrices corresponding to level  $J+1$ , that is, double sample points with a spatial discretization interval  $\Delta z^{J+1}$  (see Fig. 4). Then, we apply the one dimensional discrete wavelet transform in a successive manner to its rows and to its columns. This procedure results in a matrix composed of four submatrices arranged this way

$$\begin{bmatrix} d\sigma_1 & \gamma\sigma_1 \\ \beta\sigma_1 & \alpha\sigma_1 \end{bmatrix} = DWT_{2D}[\sigma_1]^{J+1} \quad (9.a)$$

$$\begin{bmatrix} d\sigma_2 & \gamma\sigma_2 \\ \beta\sigma_2 & \alpha\sigma_2 \end{bmatrix} = DWT_{2D}[\sigma_2]^{J+1} \quad (9.b)$$

$$\begin{bmatrix} d\sigma_1^* & \gamma\sigma_1^* \\ \beta\sigma_1^* & \alpha\sigma_1^* \end{bmatrix} = DWT_{2D}[\sigma_1^*]^{J+1} \quad (9.c)$$

$$\begin{bmatrix} d\sigma_2^* & \gamma\sigma_2^* \\ \beta\sigma_2^* & \alpha\sigma_2^* \end{bmatrix} = DWT_{2D}[\sigma_2^*]^{J+1}. \quad (9.d)$$

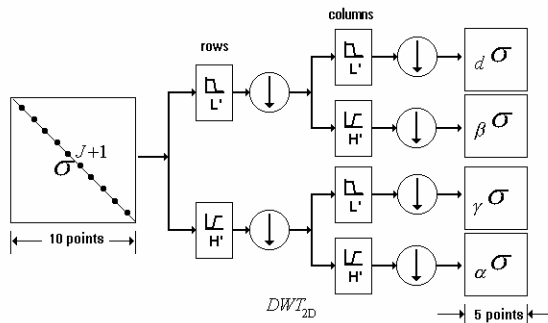


Fig. 3. Modelling of the  $\sigma$ -matrix using the two-dimensional discrete wavelet transform.

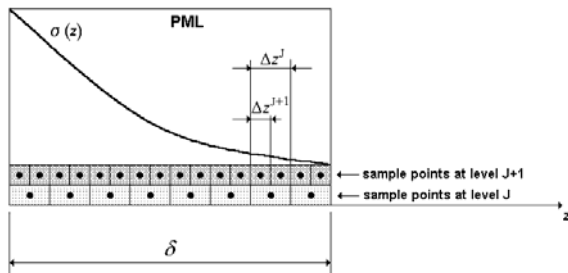


Fig. 4. Spatial discretization of the PML zone at level  $J$  and at level  $J+1$ .

### 3. NUMERICAL RESULTS

In order to evaluate the numerical effectivity of the implemented PML technique, the propagation of a TEM pulse, incident on the boundaries of the computational domain, has been simulated, and the response of the PML layer has been analyzed. A benchmark test has been done comparing the reflection coefficient  $S_{11}$  computed for three different thicknesses of the PML medium and using three different Daubechies wavelet functions ( $D_1$ ,  $D_2$ , and  $D_3$ ) in each case. The expansion of the field components with respect to space has been done using scaling and wavelet, and the time marching algorithm is then described by equations given in (8). Therefore, a numerical simulation with two levels of resolution has been done using scaling plus wavelet functions of zero order ( $J = 0$ ). We have chosen a spatial discretization interval  $\Delta z^1 = 1$  mm ( $\Delta z = 2$  mm) and a time discretization interval  $\Delta t = 3.34$  ps. The thicknesses of PML used in this test have been  $\delta = 5\Delta z$ ,  $\delta = 10\Delta z$ , and  $\delta = 15\Delta z$ . A quadratic variation in PML conductivity is assumed for all cases, with maximum theoretical reflection coefficient of  $10^{-4}$ . From equation (3), the maximum value  $\sigma_{MAX}$  obtained in each case was 3.67 S/m, 1.83 S/m, and 1.22 S/m, respectively. The reflection coefficient obtained in each case has been depicted in Figs. 5(a) through 5(c), corresponding to a PML thickness of  $5\Delta z$ ,  $10\Delta z$ , and  $15\Delta z$ , respectively. As it can be appreciated from these figures, the scheme with field components expanded in terms of Daubechies wavelet functions  $D_1$  is more sensitive to variations in the PML thickness. A great improvement is obtained with the increase of the thickness. Otherwise, the schemes with field components expanded in terms of Daubechies wavelet functions  $D_2$  and  $D_3$  are less sensitive to variations in the PML thickness and present a better behaviour than the other scheme when narrow thicknesses are used.

### 4. CONCLUSION

A procedure to implement PML absorbing boundary conditions into the MRTD scheme based on the discrete wavelet transform has been developed. This PML technique can be directly implemented into the algorithm when scaling functions are used, and for higher resolutions, the multilevel decomposition of the conductivity of the PML area needed has been done by means of the two-dimensional discrete wavelet transform. The numerical effectivity of the method has been also investigated for different thicknesses of the PML area, and using different

Daubechies wavelet functions for the expansion of the fields.

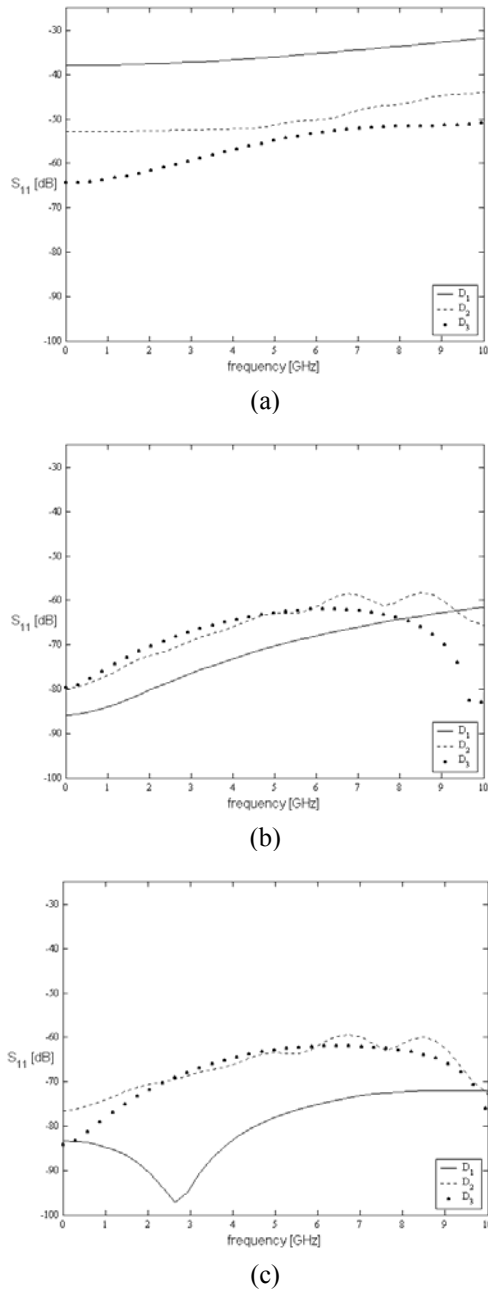


Fig. 5. Reflection coefficient  $S_{11}$  versus frequency computed using different Daubechies' wavelet functions and different thicknesses of PML: a)  $\delta=5\Delta z$ , b)  $\delta=10\Delta z$ , and c)  $\delta=15\Delta z$ .

## 5. ACKNOWLEDGEMENT

This work has been supported in part by Spanish "Comisión Interministerial de Ciencia y Tecnología". Contract/Grant number TIC2003-09677-C03-02.

## 6. REFERENCES

- [1] M. Krumpholz and L.P.B. Katehi, "MRTD: New Time-Domain schemes based on multiresolution analysis," *IEEE Trans. Microwave Theory Tech.*, vol. 44, no. 4, pp. 555–571, April 1996.
- [2] M. Fujii and W.J.R. Hoefer, "A 3-D Haar-Wavelet-Based Multiresolution Analysis Similar to the FDTD Method – Derivation and Application," *IEEE Trans. Microwave Theory Tech.*, vol. 46, no. 12, pp. 2463–2475, December 1998.
- [3] Y. W. Cheong, Y. M. Lee, K. H. Ra, and C. C. Shin, "Wavelet-Galerkin scheme of time-dependent inhomogeneous electromagnetic problems," *IEEE Microwave Guided Wave Lett.*, vol. 9, pp. 297–299, August 1999.
- [4] B. Engquist and A. Madja, "Absorbing boundary conditions for the numerical simulation of waves," *Mathematics Computation*, vol. 31, pp. 629–651, 1977.
- [5] G. Mur, "Absorbing boundary conditions for the finite-difference approximations of the time-domain electromagnetic field equations," *IEEE Trans. Electromagnetic Compatibility*, vol. 23, pp. 377–382, 1981.
- [6] K. K. Mei and J. Fang, "Superabsorption - A method to improve absorbing boundary conditions," *IEEE Trans. Antennas and Propagation*, vol. 40, pp. 1001–1010, September 1992.
- [7] J. P. Bérenger, "A perfectly matched layer for the absorption of electromagnetic waves," *J. Computational Physics*, vol. 114, pp. 185–200, 1994.
- [8] C. Represa, C. Pereira, I. Barba A.C.L. Cabeceira and J. Represa, "An approach to multiresolution in time domain based on the discrete wavelet transform," *ACES Journal*, vol. 18, no. 3, pp. 210–218, November 2003.
- [9] A. Taflove, *Computational Electrodynamics: The Finite-Difference Time-Domain Method*. Artech House, 1995.
- [10] S. G. Mallat, "A theory for multiresolution signal decomposition: The wavelet representation," *IEEE Trans. Pattern Analysis and Machine Intelligence*, vol. 11, no. 7, pp. 647–693, 1989.



**César Represa** was born in Medina del Campo, Spain, in 1971. He received the *Licenciado* degree in Physics from the University of Valladolid in 1995, and the PhD degree in 2001 from the University of Burgos. He was *Profesor Asociado* at the University of Burgos from 1997 to 2000. Since 2000 he has been

Assistant Professor at the University of Burgos. His research interest includes numerical methods in electromagnetics.



**Carmen Pereira** was born in Zamora, Spain, in 1951. She received the *Licenciado* degree in Physics in 1974, and the PhD degree in 1983, both from the University of Valladolid, Spain. She was Assistant Professor at the University of Valladolid from 1974 to 1985, and since 1985 has been *Profesor Titular*

in Electromagnetics at the Universities of Valladolid and Burgos. Her current research interest includes numerical methods in electromagnetics and microwave devices.



**Ana Cristina L. Cabeceira** was born in Pontevedra, Spain, in 1969. She received the *Licenciada* Degree on Physics in 1992, and the Ph. D. Degree in 1996, both from the University of Valladolid, Spain. From 1992 to 1999 she was Assistant Professor, then she

become *Profesora Titular* in Electromagnetism of the University of Valladolid. Her main research interests include numerical methods for Electromagnetism, as well as characterization of electromagnetics properties of materials.



**Ismael Barba** was born in Palencia, Spain, in 1970. He received his *Licenciado* degree in Physics from the University of Valladolid in 1993. He received his MA degree in Electronical Engineering in 1995, and his PhD in Physics in 1997, all from the same University. He was Assistant

Professor from 1994 to 1999, and since 1999, he is *Profesor Titular* in Electromagnetics in the University of Valladolid. His main research interest includes numerical methods in electromagnetics, and characterization of electromagnetics properties of materials.



**José Represa** was born in Valladolid, Spain, in 1953. He received the *Licenciado* degree in Physics in 1976, and the PhD degree in 1984, both from the University of Valladolid, Spain. He was Assistant Professor from 1976 to 1985, and since 1985

Professor in Electromagnetics at the University of Valladolid. His current research interest includes numerical methods in electromagnetics, characterization of electromagnetics properties of materials and microwave devices.